ASTROBIOLOGY
Volume 23, Number 6, 2023

DOI: 10.1089/ast.2022.0138

Research Articles

Open camera or QR reader and scan code to access this article and other resources online.

Detection of Short Peptides as Putative Biosignatures of Psychrophiles via Laser Desorption Mass Spectrometry

Ziqin Ni,[1] Ricardo Arevalo Jr.,[1] Anais Bardyn,[1] Lori Willhite,[1] Soumya Ray,[1] Adrian Southard,[2] Ryan Danell,[3] Jacob Graham,[4] Xiang Li,[4] Luoth Chou,[4,5] Christelle Briois,[6] Laurent Thirkell,[6] Alexander Makarov,[7] William Brinckerhoff,[4] Jennifer Eigenbrode,[4] Karen Junge,[8] and Brook L. Nunn[8]

Abstract

Studies of psychrophilic life on Earth provide chemical clues as to how extraterrestrial life could maintain viability in cryogenic environments. If living systems in ocean worlds (*e.g.,* Enceladus) share a similar set of 3-mer and 4-mer peptides to the psychrophile *Colwellia psychrerythraea* on Earth, spaceflight technologies and analytical methods need to be developed to detect and sequence these putative biosignatures. We demonstrate that laser desorption mass spectrometry, as implemented by the CORALS spaceflight prototype instrument, enables the detection of protonated peptides, their dimers, and metal adducts. The addition of silicon nanoparticles promotes the ionization efficiency, improves mass resolving power and mass accuracies via reduction of metastable decay, and facilitates peptide *de novo* sequencing. The CORALS instrument, which integrates a pulsed UV laser source and an Orbitrap™ mass analyzer capable of ultrahigh mass resolving powers and mass accuracies, represents an emerging technology for planetary exploration and a pathfinder for advanced technique development for astrobiological objectives.

Teaser: Current spaceflight prototype instrument proposed to visit ocean worlds can detect and sequence peptides that are found enriched in at least one strain of microbe surviving in subzero icy brines via silicon nanoparticle-assisted laser desorption analysis. Key Words: Laser desorption mass spectrometry—Peptide *de novo* sequencing—Biosignatures of psychrophiles. Astrobiology 23, 657–669.

1. Introduction

The search for signs of life elsewhere in the Solar System is a fundamental science goal receiving increasing attention in recent decades. Saturn's moon Enceladus and Jupiter's satellite Europa have been elevated to prime targets for astrobiology and life-detection missions in the following decades, owing to the presence of large subsurface water reservoirs (Carr *et al.,* 1998; Khurana *et al.,* 1998; Postberg *et al.,* 2011; Iess *et al.,* 2014; Glein *et al.,* 2015; McKinnon, 2015; Beuthe *et al.,* 2016; Čadek *et al.,* 2016; Thomas *et al.,* 2016; Hemingway and Mittal, 2019), active energy and material exchange across surface and interior (Smith *et al.,* 1982; Squyres *et al.,* 1983; Reynolds *et al.,* 1987; Greenberg *et al.,* 1998; Waite *et al.,* 2006, 2017; Postberg *et al.,* 2009; Patterson *et al.,* 2018), and sustained geological activity and bioavailable nutrients sufficient to power biological activities over a long period of time (Squyres *et al.,* 1983; Reynolds *et al.,* 1987; Greenberg *et al.,* 1998; Hsu *et al.,* 2015; Choblet *et al.,* 2017; Nimmo *et al.,*

[1]University of Maryland, College Park, Maryland, USA.
[2]CRESST II, College Park, Maryland, USA.
[3]Danell Consulting, Winterville, North Carolina, USA.
[4]NASA Goddard Space Flight Center, Greenbelt, Maryland, USA.
[5]Georgetown University, Washington, DC, USA.
[6]Laboratoire de Physique et Chimie de l'Environnement et de l'Espace, Orléans, France.
[7]Thermo Fisher Scientific, Bremen, Germany.
[8]University of Washington, Seattle, Washington, USA.

2018). Astrobiological objectives pertaining to these top-priority ocean worlds are not solely limited to the detection of simple organic molecules that are generic to planetary targets across the Solar System. It is strategically also important to develop capabilities to detect and recognize chemical signatures of living systems thriving in cryogenic environments akin to these potentially habitable ocean worlds (McKay *et al.,* 2008, 2014; Hendrix *et al.,* 2018; Cable *et al.,* 2021).

Proteomic studies of terrestrial extremophiles that endure some of the coldest and saltiest environments on Earth can provide chemical clues as to how extraterrestrial life could exist and maintain long-term viability under similar conditions in ocean worlds. In these hypersaline and cryogenic ecosystems, normal cellular growth and traditional metabolic and replication pathways are challenged by the limited nutrients, hypersaline conditions, and subzero temperatures. *Colwellia psychrerythraea* is an example of a marine psychrophile (*i.e.,* cold-loving bacterium) commonly found in microscopic brine pockets in Arctic sea ice. These microorganisms have evolved to survive, metabolize, and grow in polar ice (Deming and Junge, 2015) and thus may serve as biological analogs for microorganisms capable of surviving the similarly harsh conditions found on Europa and Enceladus.

In a recent experimental study, cultures of *Colwellia psychrerythraea* strain 34H (*Cp*34H) were exposed to progressively colder temperatures, higher salinities, and more depleted nutrient levels. Distinguished novel metabolic strategies responsible for maintaining viability in response to each experimental variable were identified via proteomics analysis (Mudge *et al.,* 2021). A suite of select short peptides comprising 3 or 4 amino acids (referred to as 3- and 4-mer peptides, respectively) were found to be statistically enriched in the populations that survived the harshest environmental conditions. If such enrichments are ubiquitously found in terrestrial psychrophilic organisms, then such specific 3-mers and 4-mers may represent intrinsic protective functionality. Thus, identified short peptide populations could represent putative biosignatures of psychrophiles in future efforts to search for chemical evidence of living systems in ocean worlds (Mudge *et al.,* 2021). However, such promising chemical indicators must be susceptible to analytical techniques with a path to spaceflight implementation in order to serve as practical biosignatures.

Miniaturized mass spectrometers have been developed for planetary exploration dating as far back as the Lunar Atmospheric Composition Experiment (LACE) as a part of the Apollo 17 mission in 1972 (Hoffman, 1975; Arevalo *et al.,* 2020 and references therein). In the context of astrobiology life-detection missions, spaceflight mass spectrometers have been important in the detection and identification of volatile organic and trace gases derived from the martian subsurface (Ming *et al.,* 2014; Freissinet *et al.,* 2015; Eigenbrode *et al.,* 2018; House *et al.,* 2022; Millan *et al.,* 2022), the enceladan plume (Waite *et al.,* 2006; Teolis *et al.,* 2010), and Titan's atmosphere (Niemann *et al.,* 2005). Recently, the Dragonfly Mass Spectrometer (DraMS) instrument, a dual source linear ion trap mass spectrometer that supports both gas-phase analyses and laser desorption measurements, is under development to analyze the nonvolatile organics on Titan's surface (Grubisic *et al.,* 2021). To date, no deployed mass spectrometer has analyzed a wide range of complex nonvolatile organic molecules and/or characterized their molecular structures on a flight mission. Peptides/proteins generally represent higher-fidelity indicators of living systems because their function-specific sequences and energy-optimized structures are highly unlikely to be produced abiotically (Marshall *et al.,* 2021). However, it is challenging to ionize macromolecular material via conventional spaceflight sampling and ionization methods (*e.g.,* electron ionization) and fully identify molecular compounds without the characterization of their structures.

Laser desorption mass spectrometry (LDMS) uses a focused laser beam to desorb and ionize analytes from the substrate and determines their chemical composition based on the mass-to-charge ratio (*m/z*). LDMS can desorb and ionize nonvolatile organic compounds of higher masses without incurring molecular fragmentations, allowing the determination of chemical constituents of short peptides based on their molecular masses. However, in some operational settings (such as a high laser fluence or elevated background pressure), LDMS can induce (1) characteristic cleavages of the peptide backbones during the laser irradiation in the ionization step (Köcher *et al.,* 2005; Asakawa *et al.,* 2022), (2) molecular dissociation due to collision with background neutrals (Ackloo and Loboda, 2005), and (3) breakdown of metastable ions in the ion acceleration region prior to entering the mass analyzer (Spengler *et al.,* 1991, 1992). These diagnostic fragments are informative to the peptide sequence. It would be plausible to enable simultaneous detection and sequencing of short 3-mer and 4-mer peptides in a single measurement. However, it is essential to ensure optimal ionization efficiency without incurring excessive fragmentation of the molecular ions.

To minimize molecular fragmentation during laser microprocessing, laboratories have embraced the matrix-assisted laser desorption/ionization (MALDI) technique, in which a photo-absorptive matrix compound is physically admixed with the analyte to increase the desorption and ionization efficiency (Karas *et al.,* 1987; Karas and Hillenkamp, 1988; Zenobi and Knochenmuss, 1998; Karas and Krüger, 2003). The most common MALDI matrices are solid organic acids such as α-cyano-4-hydroxycinnamic acid (α-CHCA) that are optimal for ultraviolet (UV) laser desorption/ionization (LDI). Their application enables reproducible detection and characterization of protein, peptides, oligonucleotides well over 10,000 Da at high signal-to-noise ratio (S/N) (Tanaka *et al.,* 1988). Most studies on peptide sequencing via MALDI analysis are limited to solid organic matrices due to their optimal performance and ease of laboratory technique (Spengler *et al.,* 1991, 1992; Castoro *et al.,* 1995; Chaurand *et al.,* 1999; Keough *et al.,* 1999; Hettick *et al.,* 2001; Yergey *et al.,* 2002; Köcher *et al.,* 2005). However, the breakdown of solid organic matrices, induced by laser irradiation, generates extensive fragments in the mass range $m/z < 500$, overlapping with valuable molecular species such as amino acids and peptide sequence fragments (Schmitt-Kopplin *et al.,* 2010; Leopold *et al.,* 2018). Further, the use of an organic matrix in spaceflight LDMS (1) increases the complexity of the experimental operation, such as depositing the matrix on top of the sample; (2) creates convoluted spectra by adding a wide range of low mass peaks associated with the matrix to the mass spectrum; (3) ambiguates data detection by introducing reactants to the plasma plume that may induce molecular

recombination; and (4) introduces the risk of contaminating a planetary target of astrobiological interest.

A more feasible class of MALDI matrices for spaceflight application would be inorganic material. A variety of inorganic matrices have been explored to detect biomolecules since the inception of MALDI techniques, including ultrafine metal power (Tanaka *et al.,* 1988), graphite particles in glycerol solution (Sunner *et al.,* 1995; Dale *et al.,* 1996), thin layers of activated carbon particles on an aluminum plate (Han and Sunner, 2000), and porous silicon and silica gel (Wei *et al.,* 1999; Alimpiev *et al.,* 2001; Zhang *et al.,* 2001). Silicon nanoparticles are an example of inorganic matrices that have been recently shown to promote the ionization of large organic molecules at lower fluences, improve sample homogeneity, reduce shot-to-shot variability, and suppress the salt inferences from matrices to a greater degree than neat samples (Abdelhamid, 2018; Cohen and Gusev, 2002; Wen *et al.,* 2007). Silicon nanoparticles have been applied to detect various types of small molecules, including 3-mer and 4-mer peptides, when using commercial instruments (Wen *et al.,* 2007), but they have not been used to sequence peptides. Silicon nanoparticles also have not been validated with spaceflight technologies to date. The application of inorganic matrices like silicon nanoparticles in LDMS may facilitate the detection of a wider range of molecular biosignatures in future life-detection missions, such as those complex organic molecules called out in the Europa Lander Science Definition Team Report (Hand, 2017) or the refractory organic aerosols floating in Titan's atmosphere and on Titan's surface (Cable *et al.,* 2012).

The present study aimed to investigate the feasibility of detection and *de novo* sequencing of selected 3-mer and 4-mer peptides expressed in the most resilient strains of *Cp*34H—those which are exposed to the harshest environmental conditions (Mudge *et al.,* 2021)—via the advanced prototype of CORALS (Characterization of Ocean Residues and Life Signatures), a laser desorption mass spectrometry (LDMS) instrument developed for the exploration of Europa and other ocean worlds (Briois *et al.,* 2016; Arevalo Jr. *et al.,* 2018; Willhite *et al.,* 2021). The CORALS instrument is composed of a solid-state laser system that emits 266 nm radiation (up to 450 μJ) (Fahey *et al.,* 2020) and a high-performance Orbitrap™ analyzer that can measure the *m/z* of charged analytes to the 4th decimal place. The precise and accurate measurement of *m/z* can efficiently separate ions of similar *m/z* and allows the determination of chemical constituents of unknown molecules even if they are in a sample mixture.

Our investigation began by exploring the capacity of the CORALS instrument to detect and sequence select 3-mer and 4-mer peptides in the simplest LDMS experiments, without application of any MALDI matrices. Such ''neat'' samples rely primarily on the UV absorption characteristics of the sample (and the sample plate for thin residues) to facilitate ionization of the analyte and require fewer sample handling considerations than those involving physical admixture of solid organic MALDI matrices. Early work on neat samples with the CORALS prototype demonstrated the detection of amino acids down to fmol/mm^2 concentrations and measurements of trace elements down to ppmw levels (Briois *et al.,* 2016; Arevalo Jr. *et al.,* 2018; Willhite *et al.,* 2021) but have not examined the complex refractory organic molecules. We then explored the use of silicon nanoparticles, inorganic alternatives to conventional organic compounds routinely used for MALDI techniques, to enhance ionization of the refractory organic molecules. These experiments will advance our fundamental understanding of laser desorption processes and fragmentation of relatively large organic molecules via a deep UV high-power laser. The peak distributions and fragmentation patterns obtained in each LDMS spectrum indicate plausible biosignature fingerprints expected in the search for cryogenic life in planetary environments.

2. Results

2.1. LDMS analysis of neat peptides

The peptides Ser-His-Asp (SHD) and Gly-Asp-Ala-Glu (GDAE) were 3-mer and 4-mer peptides chosen from peptides expressed in the most resilient strains of *Cp*34H that survived under the harshest environmental conditions (Mudge *et al.,* 2021). Histidine (H) is rarely found in abiotic systems and has a basic residue that has shown to improve protonation efficiency in the gas phase. Aspartic acid (D) and glutamic acid (E) have an acidic residue. SHD and GDAE were each analyzed via LDMS with the CORALS prototype (see Methods) as neat samples deposited onto a flat Al alloy plate. In the spectra collected, Cs^+ derived from a collocated finely ground disc of CsI (7.49 mm diameter) that produced by Almaz Optics, Inc. was used as an internal mass calibrant. The 3-mer SHD was identified by its protonated molecular ion (*i.e.,* $[M+H]^+$) and dimer (*i.e.,* $[2M+H]^+$), both of which were observed below the limits of quantitation (S/N < 10) despite exploring a wide range of fluences between 0.06 and 6 J/cm^2 (Fig. 1a). The most abundant organic peaks were observed up to 3 orders of magnitude lower than the intensities of Cs^+ (from the CsI disc), Al^+ (from the sample plate), and Na^+ and K^+ (from the sample solution), implying limited ionization efficiency of SHD. In contrast, GDAE was identified solely by its sodiated molecular ion (*i.e.,* $[M+Na]^+$), suggesting a distinct ionization pathway (Fig. 1b). The sodiated molecular ion was observed below the limits of quantitation, at about 2 orders of magnitude lower than the intensities of Al^+, Na^+, and K^+.

Due to the ultrahigh mass resolution and ppm-level mass accuracy provided by the CORALS analyzer, the detection of the molecular ions of SHD and GDAE enables the unambiguous determination of their respective molecular stoichiometries. However, specific diagnostic fragments are essential to reveal the entire sequence of amino acid monomers, a process known as *de novo* sequencing. Peptides are lineages of proteinogenic amino acids, which share a fundamental structure that consists of an alpha carbon ($-C_n$) at the center, bonded to an amino group ($-NH_2$), a carboxylic group (-COOH), a residue ($-R_n$) and a hydrogen atom (Fig. 2). Conventional fragmentation mechanisms induce backbone cleavages at N-C, C-C, and C-N bonds in between two consecutive amino acids. Accepted nomenclature refers to these backbone cleavages containing the N terminal of precursor peptide ions as *a-, b-,* and *c-* ions, respectively. The complementary sets of fragments containing the C terminal of the precursor peptide ions are called *x-, y-,* and *z-,* ions. A subscript *n* indicates the number of residues in the fragments, implying the location of the

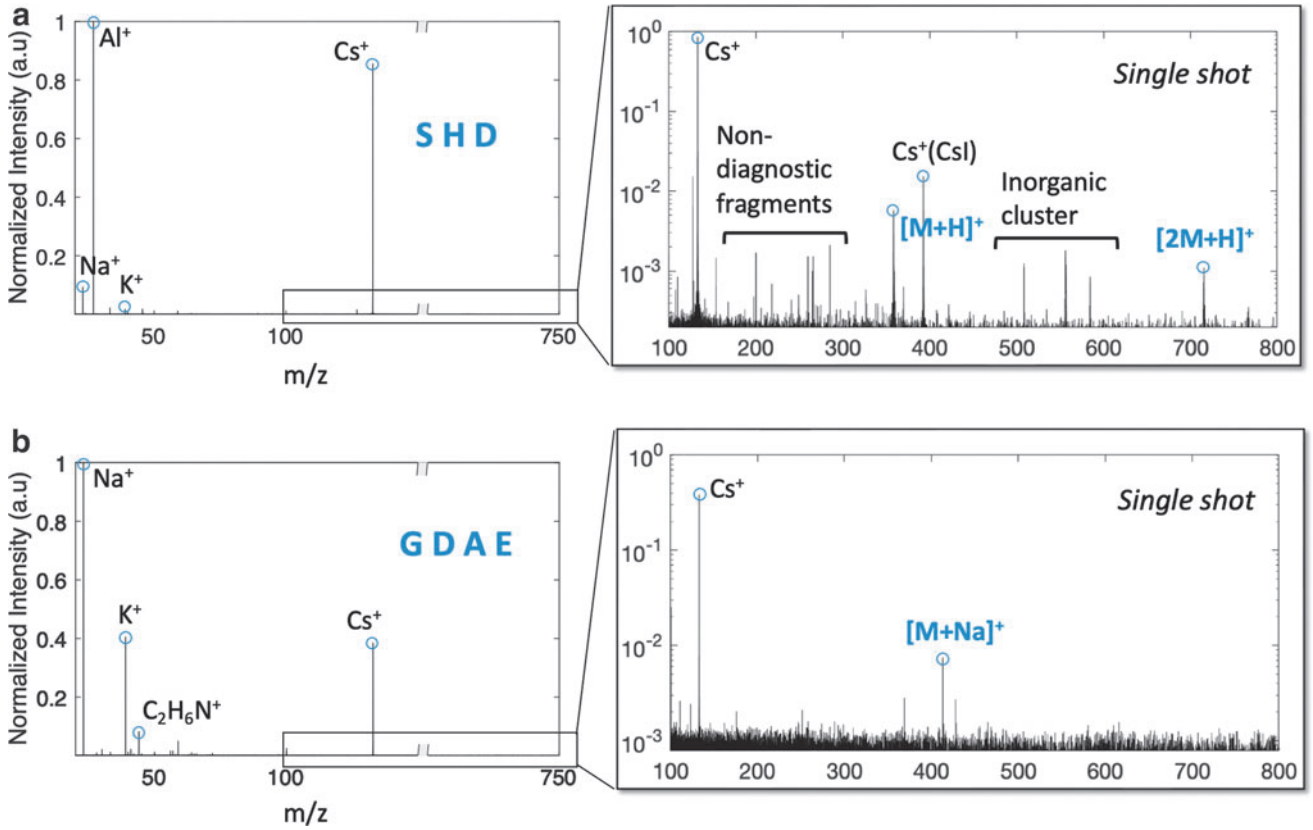

FIG. 1. Single shot LDMS analysis of neat (**a**) SHD and (**b**) GDAE on flat Al plate shows detection of molecular ions at S/N < 100 but lack of diagnostic fragments for peptide *de novo* sequencing. Spectral intensities are normalized to the maximum peak intensity observed in each scan. The characteristics of all identified peaks are listed in Supplementary Table S1. The raw transient data will be accessible in the Supplementary Material.

bond dissociation in the precursor peptide ions. This study defines *a-/x-, b-/y-, c-/z-* sequence ions as the diagnostic peptide fragments needed to achieve *de novo* sequencing. Generation of diagnostic fragments at all possible *n* locations is considered to achieve a full sequence coverage.

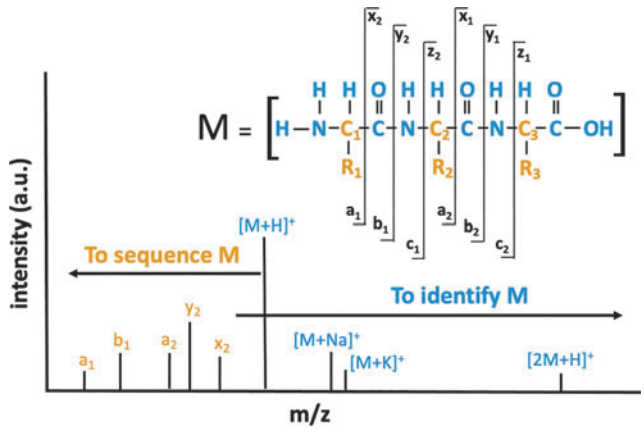

FIG. 2. A schematic diagram that shows the nomenclature of fragments in a 3-mer peptide to enable *de novo* sequencing. The alpha carbon (-C_n) and the residues (-R_n) are highlighted in the peptide structure. A list of general types of molecular adducts and diagnostic fragments is also illustrated to demonstrate the identification and sequencing of a peptide in a single mass spectrum.

Because the molecular ions of both SHD and GDAE were observed at low intensities (S/N < 100), no diagnostic fragments above the limit of detection (S/N > 3) were recorded. Although a variety of peaks were seen in the spectrum of SHD, none of them match to the exact masses of expected sequence ions. The positive mass defects of peaks in the *m/z* 150–300 range suggest the ionic species are organics composed of multiple hydrogen and nitrogen atoms. Consequently, matrix-free LDMS analysis of SHD and GDAE on an Al plate successfully demonstrates the ionization and detection of neat 3-mer and 4-mer peptides, but low sensitivities inhibit peptide *de novo* sequencing.

2.2. LDMS analysis of single peptides with silicon nanoparticles

Silicon nanoparticles serve to enhance ionization of large refractory organic molecules without excessive fragmentation. Previous studies have shown the desorption of large organic molecules at lower laser fluences with higher S/N, greater reproducibility, and with less interference from salt contamination when analyzing compounds doped with silicon nanoparticles (Abdelhamid, 2018; Cohen and Gusev, 2002; Wen *et al.,* 2007). However, to the best of our knowledge, silicon nanoparticle matrix has not yet been used to facilitate the detection and sequencing of short peptides via LDMS, nor has it been introduced to spaceflight technologies.

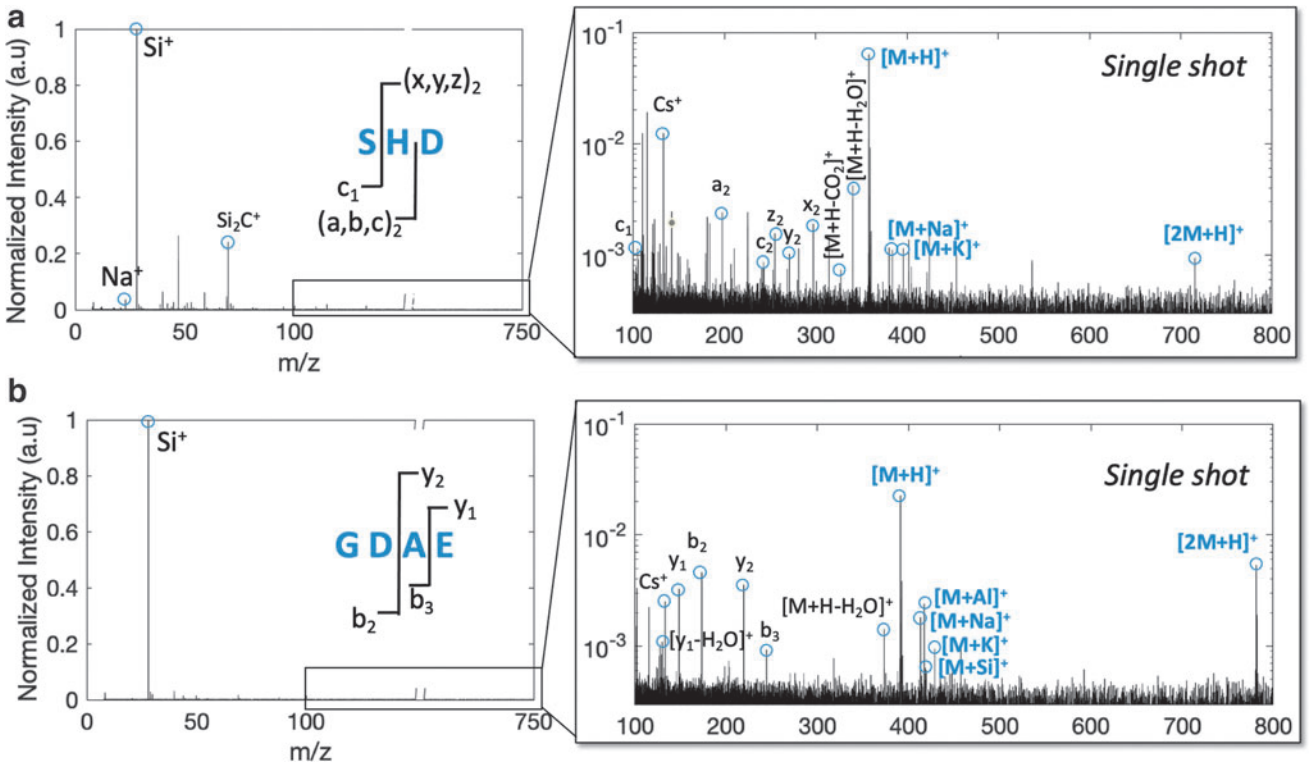

FIG. 3. Single shot LDMS analysis of neat (**a**) SHD and (**b**) GDAE on a flat Al alloy plate with silicon nanoparticles demonstrates detection of various forms of molecular ion moieties and diverse diagnostic fragments that support peptide *de novo* sequencing. Spectral intensities are normalized to the maximum peak intensity observed in each scan. The characteristics of all identified peaks are listed in Supplementary Table S1. The raw transient data will be accessible in the Supplementary Material.

To facilitate a semiquantitative comparison with the neat measurements described above, separate aliquots of SHD and GDAE were each doped with silicon nanoparticles and analyzed via LDMS with the CORALS prototype (Fig. 3). Although the highest intensity peaks in the collected spectra were sourced from the nanoparticles, the protonated molecular ions of both SHD and GDAE were observed at intensities equal to or higher than alkali metals and Al. At higher masses, protonated dimers and molecular ions with metal adducts derived from the analyte solution (*i.e.,* $[M+Na]^+$ and $[M+K]^+$), sample plate (*i.e.,* $[M+Al]^+$), and nanoparticles (*i.e.,* $[M+Si]^+$) were recorded. Dehydrated peaks derived from protonated SHD and GDAE were also observed. The exact masses of multiple molecular ions moieties provided corroborative identification of the molecular formula of each peptide.

Both peptide data sets reveal various types of diagnostic fragments. Although characteristic *b-/y-* sequence ions were observed for GDAE, access to only b_2/y_2 and b_3/y_1 provided insufficient information to sequence the entire peptide (*i.e.,* unable to distinguish GDAE or DGAE). In contrast, the spectra for SHD offered a full breadth of fragments, including c_1 and c_2 ions, successfully enabling *de novo* sequencing of SHD. Generation of various types of sequence ions at the same bond location, such as c_1 and $(x,y,z)_2$ ions generated from S-HD sequence breakage, provide redundancy to confirm the peptide sequence. Thus, these experiments corroborate the benefits of adding silicon nanoparticles to enhance the ionization efficiency of nonvolatile organic compounds, in this case short peptides, leading to improved sequencing capabilities.

2.3. LDMS of peptide mixtures with and without silicon nanoparticles

To increase the fidelity of our findings, we also explored the detectability of 3-mer and 4-mer peptides in multicomponent samples with and without silicon nanoparticles. We focused on a mixture of two peptides, Ala-Ala-Gly (AAG) and Ser-Lys-Ser-Arg (SKSR) that were statistically linked with the survivability of *Cp*34H under harsh conditions (Mudge *et al.,* 2021). Because the concentrations of both AAG and SKSR were maintained at the same level as SHD and GDAE in the single peptide experiments described above (see Methods), the two-component mixture contained twice the total concentration of peptide.

In analysis of this peptide mixture in absence of silicon nanoparticles (Fig. 4a), SKSR was identified with a diverse assortment of molecular ion moieties (*i.e.,* $[M+H]^+$, $[M+Na]^+$, and $[M+K]^+$) and a full sequence coverage. AAG was seen with various forms of molecular ions (*i.e.,* $[M+H]^+$, $[M+Al]^+$, $[M+K]^+$, and $[2M+H]^+$) and diagnostic fragments at a full peptide sequence coverage. With the addition of silicon nanoparticles (Fig. 4b), AAG was seen with a similar set of molecular ion adducts and fragmentation pattern to neat sample analysis, but SKSR was observed

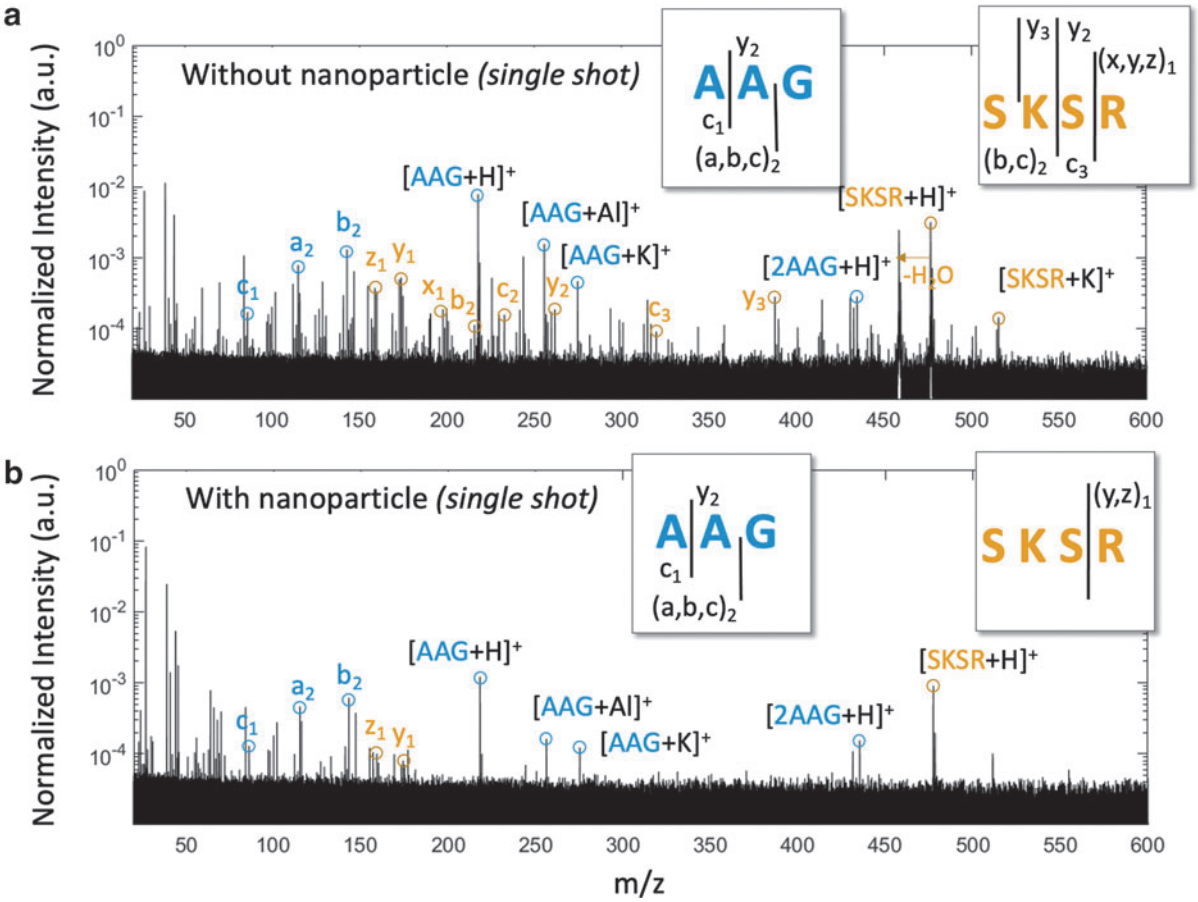

FIG. 4. Single shot LDMS analysis of peptide mixture AAG and SKSR obtained via LDMS (**a**) without nanoparticle and (**b**) with silicon nanoparticle shows detection of various forms of molecular ion adducts and diverse diagnostic fragments that support peptide *de novo* sequencing. Spectral intensities are normalized to the maximum peak intensity observed in each scan. Spectrum obtained without silicon nanoparticles was identified with a wider spread and more diverse forms of sequence ions of SKSR compared to analysis with silicon nanoparticles. The characteristics of all identified peaks are listed in Supplementary Table S1. The raw transient data will be accessible in the Supplementary Material.

with a reduced diversity of molecular ion adducts and peptide fragments (*i.e.,* y_1, z_1 are confined to proximity of arginine). Thus, the effective role of silicon nanoparticles appears to be dependent on the specific analyte(s) of interest, as discussed further below. Nonetheless, the detection of multiple molecular ion adducts and critical peptide fragments suggests that the CORALS instrument is able to discriminate, identify, and sequence SKSR and AAG simultaneously in a mixture, implying its capability to detect and characterize multiple peptides in an unknown sample from an ocean world.

3. Discussion

The data presented here demonstrate that LDMS analytical techniques, as validated by the CORALS advanced prototype instrument, enable the detection and sequencing of putative peptide biosignatures of one representative psychrophile without the application of traditional organic MALDI matrices. Distinctive species of molecular ion adducts are identified to enable peptide detection and different fragmentation mechanisms to produce peptide fragments are discussed below.

3.1. Distinctive species of molecular ion adducts to enable peptide detection

We examined a series of consecutive scans of SHD and GDAE obtained in matrix-free and matrix-assisted LDMS analysis. The molecular ion (*i.e.,* M^+) was not seen for any of the peptides examined here, with or without the application of silicon nanoparticles. This observation implies that photoionization (*i.e.,* bond gap transition via direct absorption of UV photons) is not a dominant process during LDMS analysis of 3-mer and 4-mer peptides. Most of the peptide molecules were detected as molecular ion adducts in positive ion detection mode, implying the preferred ionization pathway is to attach a proton or a cation to the analyte molecule. The sources of positively charged species could be protons derived from the solvent during sample preparation, protons transferred from analyte or matrices, residual salts from the substrate, or metals emitted from the sample plate (Jaskolla and Karas, 2011; Bae *et al.,* 2012). In particular, silicon-based inorganic matrices or substrate, such as etched porous silicon surface (Alimpiev *et al.,* 2001; Kruse *et al.,* 2001) and porous silicon powder (Zhang *et al.,* 2001), have shown to promote the protonation of analyte due to migration of proton from the surface Si-OH group as a result

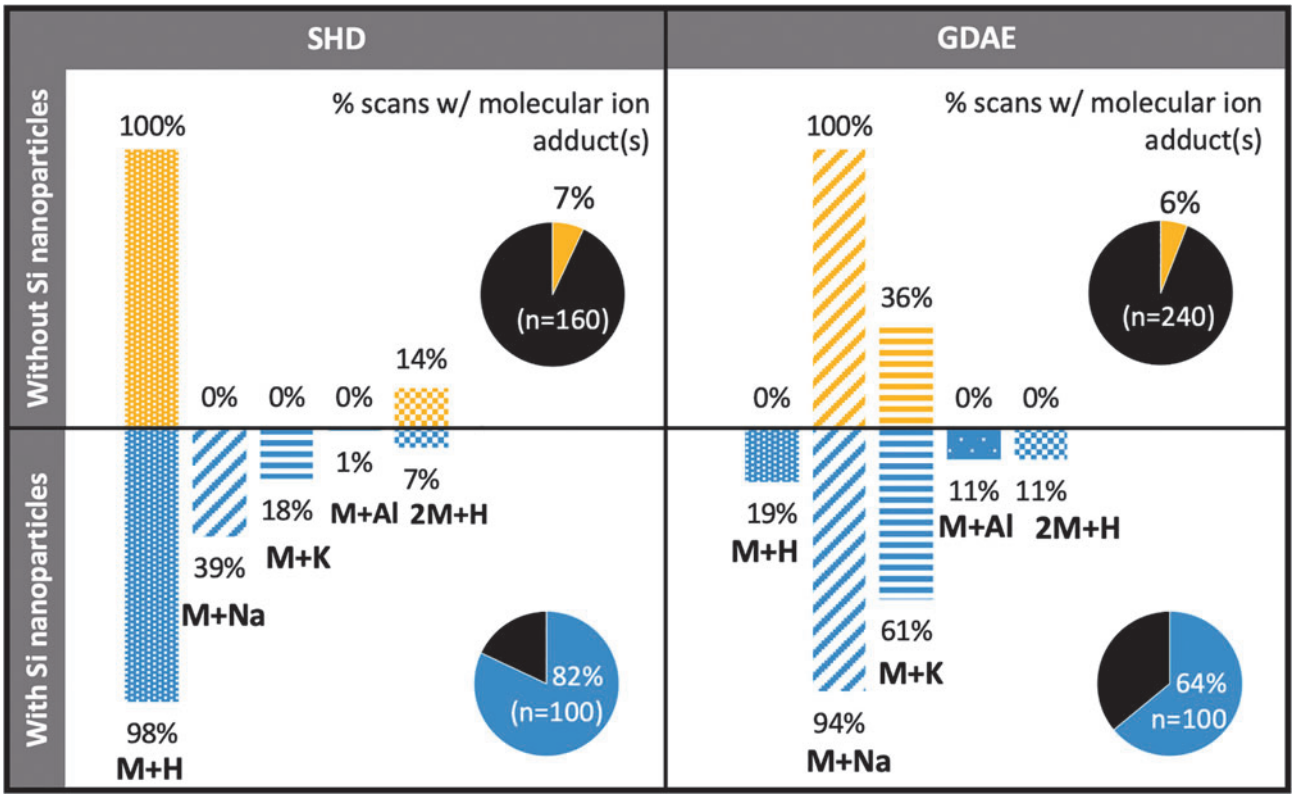

FIG. 5. The pie charts to the right of each panel summarize the percent of total scans with at least one molecular ion adduct to identify SHD and GDAE without (top) and with (below) nanoparticles. The corresponding histograms show the frequency distribution of identified molecular ion adducts among *n* number of consecutive scans.

of increasing surface acidity upon laser irradiation. Similar ionization processes could also happen to LDI analysis in the presence of silicon nanoparticles, but detailed mechanisms contributed to these ionization processes are beyond the scope of this study.

An effective scan to enable peptide detection is defined as a single-shot mass spectrum that contains at least one form of molecular ion adducts (*i.e.,* $[M+H]^+$, $[M+Na]^+$, $[M+K]^+$, $[M+Al]^+$, $[2M+H]^+$) with S/N > 3. The exact masses of target 3-mer or 4-mer peptides can be deduced from any one form of molecular ion adducts because the exact masses of proton and metals are known and have diagnostic mass defeats. Figure 5 summarized the number of effective scans in multiple consecutive single shot measurements in pie charts. The addition of silicon nanoparticles increased the rate of effective scans by 75% and 58% for SHD and GDAE, respectively. We further characterized the types of molecular ion adducts identified in each effective scan and summarized them in the corresponding histograms (Fig. 5). The compilation of matrix-free LDMS measurements revealed that only protonated SHD and cationized GDAE were observed. Such preference was maintained with addition of silicon nanoparticles and increasing types of molecular ion adducts were identified at higher S/N for both peptides. This observation suggests that, if SHD and GDAE were mixed in an unknown mixture, they would be most likely identified as protonated SHD and sodiated GDAE by the CORALS instrument. Overall, the use of silicon nanoparticles helps promote ionization efficiency, increase reproducibility of measurements, and improve surface homogeneity, so the probability of identifying SHD and GDAE in an unknown mixture would increase if silicon nanoparticles were used. This conclusion is in agreement with a previous study on small molecule analysis via MALDI with silicon nanoparticles using commercial instruments (Wen *et al.,* 2007).

3.2. Various forms of peptide fragments to enable *de novo* sequencing

Electron transfer/capture dissociation (ETD or ECD), ultraviolet photodissociation (UVPD), and collision-induced dissociation (CID) are three primary dissociation methods used in conventional tandem mass spectrometry to achieve peptide *de novo* sequencing. Similar charge-driven, collision-induced, and photon-activated dissociation could have occurred during LDI measurements. Observation of ETD/ECD-like and CID-like fragments, as well as UVPD-specific fragments, provides insights into mechanisms associated with the peptide fragmentation prior to entering the mass analyzers.

Electron transfer/capture dissociation–like fragments, or *c-/z-* sequence ions, have been observed in this study, suggesting that charges are introduced to trigger peptide fragmentation during LDI measurements (Syka *et al.,* 2004). Potential sources of charges in the ionization source include electrons in the plume (Karas *et al.,* 2000; Nielsen *et al.,* 2003), plasmon-induced electrons on the metal plate surface

or metallic nanoparticles (Mukherjee *et al.,* 2013; Clavero, 2014; Szczerbiński *et al.,* 2020), and/or hydrogen radicals derived from solvents or matrices (Köcher *et al.,* 2005; Demeure *et al.,* 2010). Though this study is incapable of distinguishing the primary donor of charges during LDI analysis, observation of *c-/z-* sequence ions in measurements with and without matrices suggests charge-driven dissociation is not limited to the silicon nanoparticles itself. The use of silicon nanoparticles does not strongly favor the generation of *c-/z-* sequence ions, like some of the solid organic matrices (*e.g.,* 1,5-DAN) would do due to their high yields of hydrogen radical production (Memboeuf *et al.,* 2010).

Ultraviolet photodissociation–specific fragments, or *a-/x-* sequence ions, are observed at S/N > 10, suggesting that peptide molecules dissociate as they interact with 266 nm radiation. In analysis of peptide mixture AAG and SKSR studied here, *a-/x-* sequence ions are identified exclusively to AAG, but no such fragments were identified for SKSR, suggesting the effectiveness of UVPD is specific to analytes themselves, especially their UV absorbance. The use of silicon nanoparticles promotes the generation of UVPD-specific fragments from AAG.

Collision-induced dissociation–like fragments, namely *a-, b-,* and *y-* sequence ions, are the dominant sequence ions observed in this study, suggesting that thermal dissociation plays a critical role to fragment peptides via LDI analyses (Falick *et al.,* 1993; Medzihradszky *et al.,* 2000). Peptide molecular ions could be thermally activated by ion-neutral collisions in the ionization source. Ion-neutral collisions have been observed at the front of expanding laser-induced plasma plumes via fast photography (Gusarov *et al.,* 2000; Kushwaha and Thareja, 2008; Valverde *et al.,* 2014), suggesting CID-like fragments could be generated as the expanding plume materials collide with the background neutrals in atmospheric pressure. Similar effects albeit at a much lower pressure level occur upon expansion into vacuum (Spengler *et al.,* 1991).

Peptide molecular ions could also be thermally activated by the heat conducted from the UV-absorbing silicon nanoparticles and/or the Al alloy sample plate. Controlled amount of thermal energy absorbed by molecular ions can facilitate desorption of intact molecules and produce CID-like fragments to facilitate peptide *de novo* sequencing (Kim *et al.,* 2012, 2013). These fragments were generated from metastable decay and were shown with reduced spectral resolution due to peak broadening and low S/N (Spengler *et al.,* 1991). If the thermal energy is excessive, dissociation of protonated peptides could occur at any bond via an energy randomization process, generating a sea of fragments that are not unique to the peptide backbone nor comply to commonly accepted mobile proton frameworks, and even generation of recombination products as the plume cools (Wysocki *et al.,* 2000; Paizs and Suhai, 2005). For example, the nondiagnostic fragments and inorganic clusters observed in the neat analysis of SHD challenge spectral interpretation and hamper peptide *de novo* sequencing. Therefore, optimal performance of peptide detection and sequencing via LDMS analysis requires active control of thermal-induced molecular desorption and breakdown.

Silicon nanoparticles appear to be an effective matrix to facilitate the reproducible formation of molecular ion adducts at increasing S/N and reduced metastable fragmentation. Future work needs to explore how different inorganic matrices (*e.g.,* nanoparticle versus nanowire, distinct composition, particle size distribution) control ionization efficiency, sensitivity, and fragmentation potential for specific classes of molecules. Different data acquisition and data processing strategies should be explored to maximize science return given the limited data storage and processing power onboard; for example, summing multiple scans can reduce noise floor and improve the detection limits when time and energy are available, and use of machine learning algorithms to extract and identify molecules from sample mixtures (Theiling *et al.,* 2022). Based on findings present here, a notional concept of operation for an astrobiology landed mission to a cryogenic ocean world might include sample acquisition, deposition, and sublimation of icy samples onto a suite of sample plates preloaded with a variety of inorganic matrices. The sensitivity of analytical measurements could be further enhanced if the icy samples were preprocessed using hyphenated separation techniques (such as electrophoresis) prior to sample deposition on the metal plate.

In summary, this study demonstrates successful peptide identification via simple LDMS techniques, and *de novo* sequencing of select peptides with the addition of silicon nanoparticles. Coupled to a high-power UV laser, the silicon nanoparticles enhanced ionization efficiency and promoted the generation of diagnostic *b-/y-/a-* sequence ions in a single scan, similar to CID techniques. This preliminary analysis opens the door for future investigations into peptide detection and sequencing via inorganic matrices like silicon nanoparticles, alternatives to conventional solid organic matrices that are incompatible with planetary protection measures and represent risks for forward contamination for missions to astrobiological destinations.

Further, this study showcases the analytical capabilities of spaceflight prototype CORALS to detect and sequence putative peptide biosignatures of psychrophiles for *in situ* investigation of ocean worlds. Even with the simplest sample preparation method, a single spectrum collected from the CORALS prototype reveals (1) various forms of molecular ion adducts across a wide mass range, providing for robust identification and cross-validation to the chemical composition of molecular ions with high mass accuracy measurements; (2) diagnostic peptide fragments at a full sequence coverage adequate to elucidate the monomer sequence in samples with silicon nanoparticles added; (3) improved resolution and mass accuracy due to reduction of metastable decay with silicon nanoparticles. The benefits of incorporating silicon or other metal/metalloid nanoparticles into LDMS techniques could increase the science return of future spaceflight investigations.

4. Materials and Methods

4.1. Peptide selection and preparation

A subset of psychrophilic peptides was selected to demonstrate the detection and identification of molecular ions and diagnostic fragments at higher laser energy with the CORALS instrument. These four different short peptides are Ala-Ala-Gly (AAG) (monoisotopic mass: 217.1062), Ser-His-Asp (SHD) (monoisotopic mass: 357.1284), Gly-Asp-Ala-Glu (GDAE) (monoisotopic mass: 390.1387),

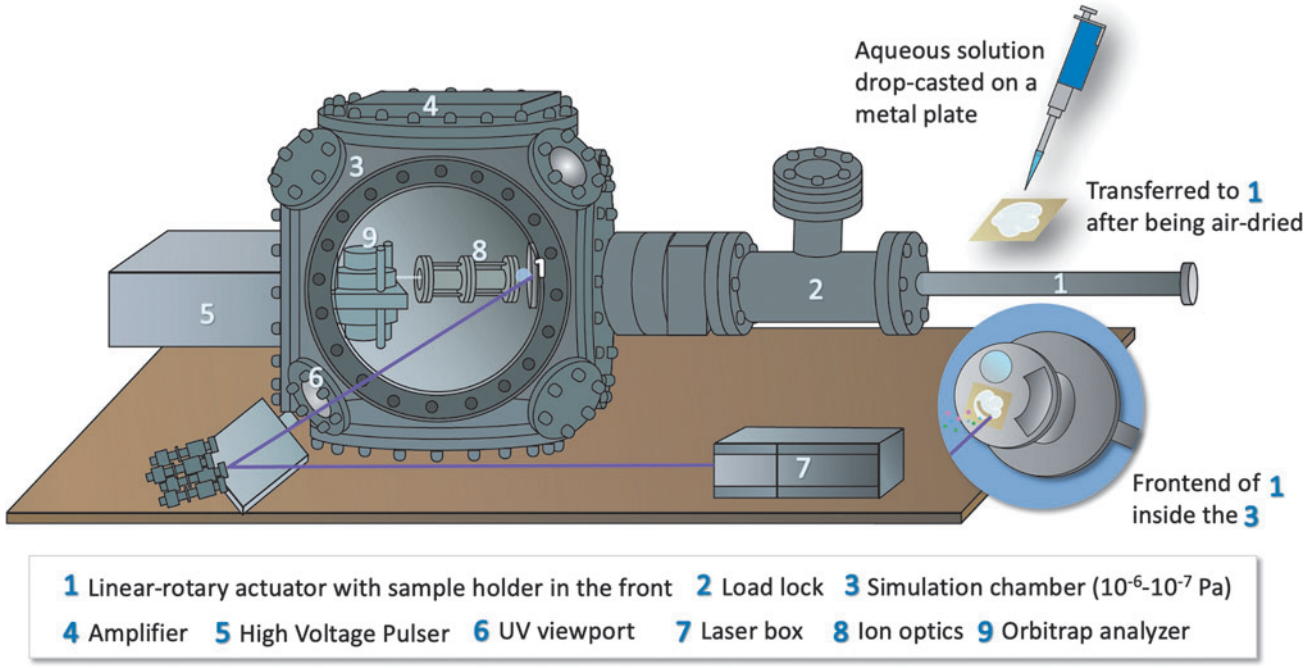

FIG. 6. Sample preparation and instrument setup at NASA Goddard Space Flight Center.

Ser-Lys-Ser-Arg (SKSR) (monoisotopic mass: 477.2707). These four peptides were selected because they constitute amino acids of different basicity. Aspartic acid and glutamic acid have acidic side chains, while arginine, histidine, and lysine have basic side chains. The selected peptides have a mixture of amino acids of different weights and sizes. High-molecular-weight amino acids like histidine are rarely found in abiotic systems, while low-molecular-weight amino acids like glycine and alanine have been found in high abundance in meteorites and are thus more likely to be used as starting materials to construct functional polymers (Wen *et al.*, 2007). These peptides were synthesized from Biomatik with purity >95%. Each peptide was dissolved in 0.1 wt % formic acid solution (Fisher Chemical, ≥99.0%) to form ~5 wt % peptide stock solutions, and they were used without further purification.

Matrix-free peptide samples: About 200 uL of aqueous solution was directly drop-cast on the aluminum (Al) alloy metal plate (Goodfellow AL7075 foil) to form a droplet of ~60 mm^2 in size and achieve surface analyte concentration ~5e5 pmol/mm^2. The Al alloy plate was pretreated with acetone and isopropyl alcohol. The droplet was allowed to dry on the hotplate at 75°C until a thin residue of peptide was formed on the Al alloy plate. The plate was then transferred and taped on the stainless-steel sample target, ready for sample introduction to the CORALS prototype instrument at NASA Goddard Space Flight Center. Though such sample preparation method does not create a homogeneous surface for quantitative measurements, it is representative of realistic sample handling and preparation during *in situ* investigation of icy worlds.

Matrix-assisted peptide samples: The silicon nanoparticles were purchased from Sigma-Aldrich (<100 nm particle size, ≥98% trace metals basis) and used without further purification. Acetone (Sigma-Aldrich, ≥99.5%) was used to mix with a few mg of the silicon nanoparticles to form a liquid slurry. A total of 2 uL of the slurry was deposited onto the sample plate and dried, forming a very thin layer of the nano powder on the surface. The peptide solution then was deposited on top of the nanoparticle layer and dried. Because of the high volatility of acetone in the room temperature, acetone would be completely evaporated before the sample was introduced to the instrument. No signature of acetone has been observed in the mass spectra.

4.2. Instrument setup

The sample was analyzed by the CORALS prototype instrument at NASA Goddard Space Flight Center (Fig. 6). The CORALS prototype (60×45×45 cm) is composed of a breadboard of the CORALS laser, integrated to an Orbitrap analyzer and a custom-built ion inlet assembly through a Kimball Physics vacuum chamber. The chamber maintains its low-pressure condition at typically ≤10^{-6}–10^{-7} Pa, and the pressure is monitored by a high-vacuum cold-cathode vacuum gauge. Sample plate is introduced into the low-pressure simulation chamber through a load lock via a linear-rotary actuator. The laser beam enters the simulation chamber through a deep UV viewport that offers high transmission of 266 nm radiation and irradiates the sample at a 45° angle. Ions generated from the sample plate are propelled by a high voltage supplied to the sample plate, collimated by the ion optics, accelerated, and injected into the mass analyzer. The image current induced by ions oscillating inside the Orbitrap was detected, amplified, digitized, and exported for offline data processing. All instrument control, voltage and timing tuning, and data acquisition is accomplished with custom LabVIEW-based software (RITS, Danell Consulting, Inc.) (Danell, 2010).

4.3. Data collection and processing

Each transient spectrum (200 ms in length) was collected at a sampling rate of 5 MHz and then processed to generate a frequency spectrum via Fast Fourier Transform (FFT) in MATLAB. Three times zero-filling to $3X + N = 2^Y$ (where X is the original transient length, N the remaining amount needed to achieve the nearest power of 2, and Y the final zero-filled transient length) was applied prior to FFT to improve peak shape and mass accuracy. No apodization was applied to the transient prior to FFT analysis, and the reasons have been discussed in supplementary notes. The frequency spectrum was calibrated into a mass spectrum using an internal standard, typically Cs^+ or Al^+. Identified peaks were fitted with a gaussian distribution using Origin (OriginLab Corporation). The derived peak height, peak width, and center mass are used to calculate S/N, mass resolution, and mass accuracy, respectively. Peak identification and characterization are reported in the Supplementary Material.

Acknowledgments

We appreciate the thorough review from Paul Mahaffy. This study was supported financially by NASA ROSES ICEE 2 Grant 80NSSC19K0610, ROSES DALI Grant 80NSSC19K0768, and GSFC Grant 80NSSC18K1612. LC was supported by an appointment to the NASA Postdoctoral Program at the NASA Goddard Space Flight Center administered by USRA and ORAU through a contract with NASA, by the NASA-funded Laboratory for Agnostic Biosignatures Project (NASA Grant 80NSSC18K1140), and by the Mars Science Laboratory mission.

Supplementary Material

Supplementary Text
Supplementary Figure S1
Supplementary Table S1

References

Abdelhamid HN. Nanoparticle assisted laser desorption/ionization mass spectrometry for small molecule analytes. *Microchim Acta* 2018;185(3):200; doi: 10.1007/s00604-018-2687-8.

Ackloo S, Loboda A. Applications of a matrix-assisted laser desorption/ionization orthogonal time-of-flight mass spectrometer. L. Metastable decay and collision-induced dissociation for sequencing peptides. *Rapid Commun Mass Spectrom* 2005;19(2):213–220; doi: 10.1002/rcm.1775.

Alimpiev S, Nikiforov S, Karavanskii V, *et al.* On the mechanism of laser-induced desorption–ionization of organic compounds from etched silicon and carbon surfaces. *J Chem Phys* 2001;115(4):1891–1901; doi: 10.1063/1.1381531.

Arevalo Jr. R, Selliez L, Briois C, *et al.* An Orbitrap-based laser desorption/ablation mass spectrometer designed for spaceflight. *Rapid Commun Mass Spectrom* 2018;32(21):1875–1886; doi: 10.1002/rcm.8244.

Arevalo R, Ni Z, Danell RM. Mass spectrometry and planetary exploration: A brief review and future projection. *J Mass Spectrom* 2020;55(1):e4454; doi: 10.1002/jms.4454

Asakawa D, Hosokai T, Nakayama Y. Experimental and theoretical investigation of MALDI in-source decay of peptides with a reducing matrix: What is the initial fragmentation step? *J Am Soc Mass Spectrom* 2022;33(6):1011–1021; doi: 10.1021/jasms.2c00066.

Bae YJ, Shin YS, Moon JH, *et al.* Degree of ionization in MALDI of peptides: Thermal explanation for the gas-phase ion formation. *J Am Soc Mass Spectrom* 2012;23(8):1326–1335; doi: 10.1007/s13361-012-0406-y

Beuthe M, Rivoldini A, Trinh A. Enceladus's and Dione's floating ice shells supported by minimum stress isostasy. *Geophys Res Lett* 2016;43(19):10088–10096; doi: 10.1002/2016GL070650.

Briois C, Thissen R, Thirkell L, *et al.* Orbitrap mass analyser for *in situ* characterisation of planetary environments: Performance evaluation of a laboratory prototype. *Planet Space Sci* 2016;131:33–45; doi: 10.1016/j.pss.2016.06.012.

Cable ML, Hörst SM, Hodyss R, *et al.* Titan tholins: Simulating Titan organic chemistry in the Cassini-Huygens era. *Chem Rev* 2012;112(3):1882–1909; doi: 10.1021/cr200221x.

Cable ML, Porco C, Glein CR, *et al.* The science case for a return to Enceladus. *Planet Sci J* 2021;2(4):132; doi: 10.3847/PSJ/abfb7a.

Čadek O, Tobie G, Van Hoolst T, *et al.* Enceladus's internal ocean and ice shell constrained from Cassini gravity, shape, and libration data. *Geophys Res Lett* 2016;43(11):5653–5660; doi: 10.1002/2016GL068634.

Carr MH, Belton MJS, Chapman CR, *et al.* Evidence for a subsurface ocean on Europa. *Nature* 1998;391:363–365; doi: 10.1038/34857.

Castoro JA, Wilkins CL, Woods AS, *et al.* Peptide amino acid sequence analysis using matrix-assisted laser desorption/ionization and Fourier transform mass spectrometry. *J Mass Spectrom* 1995;30(1):94–98; doi: 10.1002/jms.1190300115.

Chaurand P, Luetzenkirchen F, Spengler B. Peptide and protein identification by matrix-assisted laser desorption ionization (MALDI) and MALDI-post-source decay time-of-flight mass spectrometry. *J Am Soc Mass Spectrom* 1999;10(2):91–103; doi: 10.1016/S1044-0305(98)00145-7.

Choblet G, Tobie G, Sotin C, *et al.* Powering prolonged hydrothermal activity inside Enceladus. *Nat Astron* 2017;1:841–847; doi: 10.1038/s41550-017-0289-8.

Clavero C. Plasmon-induced hot-electron generation at nanoparticle/metal-oxide interfaces for photovoltaic and photocatalytic devices. *Nat Photonics* 2014;8(2):95–103; doi: 10.1038/nphoton.2013.238.

Cohen LH, Gusev AI. Small molecule analysis by MALDI mass spectrometry. *Anal Bioanal Chem* 2002;373(7):571–586; doi: 10.1007/s00216-002-1321-z.

Dale MJ, Knochenmuss R, Zenobi R. Graphite/Liquid mixed matrices for laser desorption/ionization mass spectrometry. *Anal Chem* 1996;68(19):3321–3329; doi: 10.1021/ac960558i.

Danell R. A full featured, flexible, and inexpensive 2D and 3D ion trap control architecture and software package. In *Proceedings of the 58th ASMS Conference on Mass Spectrometry and Allied Topics*. American Society for Mass Spectrometry: Santa Fe, NM; 2010.

Demeure K, Gabelica V, De Pauw EA. New advances in the understanding of the in-source decay fragmentation of peptides in MALDI-TOF-MS. *J Am Soc Mass Spectrom* 2010;21(11):1906–1917; doi: 10.1016/j.jasms.2010.07.009

Deming JW, Junge K. *Colwellia.* In *Bergey's Manual of Systematics of Archaea and Bacteria*. In (Vol. 410. Whitman WB. ed.) Wiley: Hoboken, NJ, 2015; pp 1–12.

Eigenbrode JL, Summons RE, Steele A, *et al.* Organic matter preserved in 3-billion-year-old mudstones at Gale Crater, Mars. *Science* 2018;360(6393):1096–1101; doi: 10.1126/science.aas9185.

Fahey M, Yu A, Grubisic A, *et al.* Ultraviolet laser development for planetary lander missions. In *2020 IEEE Aerospace Conference*. IEEE, Piscataway, NJ, 2020; doi: 10.1109/AERO47225.2020.9172711.

Falick AM, Hines WM, Medzihradszky KF, *et al.* Low-mass ions produced from peptides by high-energy collision-induced dissociation in tandem mass spectrometry. *J Am Soc Mass Spectrom* 1993;4(11):882–893; doi: 10.1016/1044-0305(93)87006-X.

Freissinet C, Glavin DP, Mahaffy PR, *et al.* Organic molecules in the Sheepbed Mudstone, Gale Crater, Mars. *J Geophys Res Planets* 2015;120(3):495–514; doi: 10.1002/2014JE004737.

Glein CR, Baross JA, Waite JH. The pH of Enceladus' ocean. *Geochim Cosmochim Acta* 2015;162:202–219; doi: 10.1016/j.gca.2015.04.017.

Greenberg R, Geissler P, Hoppa G, *et al.* Tectonic processes on Europa: Tidal stresses, mechanical response, and visible features. *Icarus* 1998;135(1):64–78; doi: 10.1006/icar.1998.5986.

Grubisic A, Trainer M, Li X, *et al.* Laser desorption mass spectrometry at Saturn's moon Titan. *Int J Mass Spectrom* 2021;470:116707; doi: 10.1016/j.ijms.2021.116707.

Gusarov AV, Gnedovets AG, Smurov I. Gas dynamics of laser ablation: Influence of ambient atmosphere. *J Appl Phys* 2000;88(7):4352; doi: 10.1063/1.1286175.

Han M, Sunner J. An activated carbon substrate surface for laser desorption mass spectrometry. *J Am Soc Mass Spectrom* 2000;11(7):644–649; doi: 10.1016/S1044-0305(00)00129-X.

Hand KP. *Europa Lander Study 2016 Report.* (JPL D-97667) NASA: Washington, DC; 2017; https://europa.nasa.gov/resources/58/europa-lander-study-2016-report [Last accessed: 3/24/2023].

Hemingway DJ, Mittal T. Enceladus's ice shell structure as a window on internal heat production. *Icarus* 2019;332:111–131; doi: 10.1016/j.icarus.2019.03.011.

Hendrix AR, Hurford TA, Barge LM, *et al.* The NASA Roadmap to Ocean Worlds. *Astrobiology* 2018;19(1):1–27; doi: 10.1089/ast.2018.1955.

Hettick JM, McCurdy DL, Barbacci DC, *et al.* Optimization of sample preparation for peptide sequencing by MALDI-TOF photofragment mass spectrometry. *Anal Chem* 2001;73(22):5378–5386; doi: 10.1021/ac0102157.

Hoffman JH. *Lunar Atmospheric Composition Experiment. Final Report, 1 Jun. 1971—30 Sep. 1975*. (N-76-32089; NASA-CR-150946.) Richardson Center for Advanced Studies, Texas University: Dallas, TX; 1975.

House CH, Wong GM, Webster CR, *et al.* Depleted carbon isotope compositions observed at Gale Crater, Mars. *Proc Natl Acad Sci USA* 2022;119(4):e2115651119; doi: 10.1073/pnas.2115651119.

Hsu H-W, Postberg F, Sekine Y, *et al.* Ongoing hydrothermal activities within Enceladus. *Nature* 2015;519:7542; doi: 10.1038/nature14262.

Iess L, Stevenson DJ, Parisi M, *et al.* The gravity field and interior structure of Enceladus. *Science* 2014;344(6179):78–80; doi: 10.1126/science.1250551.

Jaskolla TW, Karas M. Compelling evidence for lucky survivor and gas phase protonation: The Unified MALDI Analyte Protonation Mechanism. *J Am Soc Mass Spectrom* 2011;22(6):976–988; doi: 10.1007/s13361-011-0093-0.

Karas M, Hillenkamp F. Laser desorption ionization of proteins with molecular masses exceeding 10,000 daltons. *Anal Chem* 1988;60(20):2299–2301; doi: 10.1021/ac00171a028.

Karas M, Krüger R. Ion formation in MALDI: The cluster ionization mechanism. *Chem Rev* 2003;103(2):427–440; doi: 10.1021/cr010376a.

Karas M, Bachmann D, Bahr U, *et al.* Matrix-assisted ultraviolet laser desorption of non-volatile compounds. *Int J Mass Spectrom Ion Process* 1987;78:53–68; doi: 10.1016/0168-1176(87)87041-6.

Karas M, Glückmann M, Schäfer J. Ionization in matrix-assisted laser desorption/ionization: Singly charged molecular ions are the lucky survivors. *J Mass Spectrom* 2000;35(1):1–12; doi: 10.1002/(SICI)1096-9888(200001)35:1<1::AID-JMS904>3.0.CO;2-0.

Keough T, Youngquist RS, Lacey MP. A method for high-sensitivity peptide sequencing using postsource decay matrix-assisted laser desorption ionization mass spectrometry. *Proc Natl Acad Sci USA* 1999;96(13):7131–7136; doi: 10.1073/pnas.96.13.7131.

Khurana KK, Kivelson MG, Stevenson DJ, *et al.* Induced magnetic fields as evidence for subsurface oceans in Europa and Callisto. *Nature* 1998;395:6704; doi: 10.1038/27394.

Kim SH, Lee A, Song JY, *et al.* Laser-induced thermal desorption facilitates postsource decay of peptide ions. *J Am Soc Mass Spectrom* 2012;23(5):935–941; doi: 10.1007/s13361-012-0355-5.

Kim SH, Kim J, Moon DW, *et al.* Commercial silicon-on-insulator (SOI) wafers as a versatile substrate for laser desorption/ionization mass spectrometry. *J Am Soc Mass Spectrom* 2013;24(1):167–170; doi: 10.1007/s13361-012-0534-4.

Köcher T, Engström Å, Zubarev RA. Fragmentation of peptides in MALDI in-source decay mediated by hydrogen radicals. *Anal Chem* 2005;77(1):172–177; doi: 10.1021/ac0489115.

Kruse RA, Li X, Bohn PW, *et al.* Experimental factors controlling analyte ion generation in laser desorption/ionization mass spectrometry on porous silicon. *Anal Chem* 2001;73(15):3639–3645; doi: 10.1021/ac010317x.

Kushwaha A, Thareja RK. Dynamics of laser-ablated carbon plasma: Formation of C_2 and CN. *Appl Opt* 2008;47(31):G65; doi: 10.1364/AO.47.000G65.

Leopold J, Popkova Y, Engel KM, *et al.* Recent developments of useful MALDI matrices for the mass spectrometric characterization of lipids. *Biomolecules* 2018;8(4):173; doi: 10.3390/biom8040173.

Marshall SM, Mathis C, Carrick E, *et al.* Identifying molecules as biosignatures with assembly theory and mass spectrometry. *Nat Commun* 2021;12:1; doi: 10.1038/s41467-021-23258-x.

McKay CP, Porco CC, Altheide T, *et al.* The possible origin and persistence of life on Enceladus and detection of biomarkers in the plume. *Astrobiology* 2008;8(5):909–919; doi: 10.1089/ast.2008.0265.

McKay CP, Anbar AD, Porco C, *et al.* Follow the plume: The habitability of Enceladus. *Astrobiology* 2014;14(4):352–355; doi: 10.1089/ast.2014.1158.

McKinnon WB. Effect of Enceladus's rapid synchronous spin on interpretation of Cassini gravity. *Geophys Res Lett* 2015;42(7):2137–2143; doi: 10.1002/2015GL063384.

Medzihradszky KF, Campbell JM, Baldwin MA, *et al.* The characteristics of peptide collision-induced dissociation using a high-performance MALDI-TOF/TOF tandem mass spectrometer. *Anal Chem* 2000;72(3):552–558; doi: 10.1021/ac990809y.

Memboeuf A, Nasioudis A, Indelicato S, *et al.* Size effect on fragmentation in tandem mass spectrometry. *Anal Chem* 2010;82(6):2294–2302; doi: 10.1021/ac902463q.

Millan M, Teinturier S, Malespin CA, *et al.* Organic molecules revealed in Mars's Bagnold Dunes by Curiosity's derivatization experiment. *Nat Astron* 2022;6:1; doi: 10.1038/s41550-021-01507-9.

Ming DW, Archer PD, Glavin DP, *et al.* Volatile and organic compositions of sedimentary rocks in Yellowknife Bay, Gale Crater, Mars. *Science*, 2014;343:6169; doi: 10.1126/science.1245267.

Mudge MC, Nunn BL, Firth E, *et al.* Subzero, saline incubations of *Colwellia psychrerythraea* reveal strategies and biomarkers for sustained life in extreme icy environments. *Environ Microbiol* 2021;23(7):3840–3866; doi: 10.1111/1462-2920.15485.

Mukherjee S, Libisch F, Large N, *et al.* Hot electrons do the impossible: Plasmon-induced dissociation of H_2 on Au. *Nano Letters* 2013;13(1):240–247; doi: 10.1021/nl303940z.

Nielsen ML, Budnik BA, Haselmann KF, *et al.* Tandem MALDI/EI ionization for tandem Fourier transform ion cyclotron resonance mass spectrometry of polypeptides. *Int J Mass Spectrom* 2003;226(1):181–187; doi: 10.1016/S1387-3806(02)00970-3.

Niemann HB, Atreya SK, Bauer SJ, *et al.* The abundances of constituents of Titan's atmosphere from the GCMS instrument on the Huygens probe. *Nature* 2005;438:7069; doi: 10.1038/nature04122.

Nimmo F, Barr AC, Běhounkova M, *et al.* The thermal and orbital evolution of Enceladus: Observational constraints and models. In *Enceladus and the Icy Moons of Saturn*. (Schenk PM, Clark RN, Howett JA, *et al.* eds.) University of Arizona Press: Tucson, 2018; pp 79–94.

Paizs B, Suhai S. Fragmentation pathways of protonated peptides. *Mass Spectrom Rev* 2005;24(4):508–548; doi: 10.1002/mas.20024.

Patterson GW, Kattenhorn SA, Helfenstein P, *et al.* The geology of Enceladus. In *Enceladus and the Icy Moons of Saturn*. (Schenk PM, Clark RN, Howett JA, *et al.* eds.) University of Arizona Press: Tucson, 2018; pp 95–126.

Postberg F, Kempf S, Schmidt J, *et al.* Sodium salts in E-ring ice grains from an ocean below the surface of Enceladus. *Nature* 2009;459:7250; doi: 10.1038/nature08046.

Postberg F, Schmidt J, Hillier J, *et al.* A salt-water reservoir as the source of a compositionally stratified plume on Enceladus. *Nature* 2011;474(7353):620–622; doi: 10.1038/nature10175.

Reynolds RT, McKay CP, Kasting JF. Europa, tidally heated oceans, and habitable zones around giant planets. *Adv Space Res* 1987;7(5):125–132; doi: 10.1016/0273-1177(87)90364-4.

Schmitt-Kopplin P, Gabelica Z, Gougeon RD, *et al.* High molecular diversity of extraterrestrial organic matter in Murchison meteorite revealed 40 years after its fall. *Proc Natl Acad Sci USA* 2010;107(7):2763–2768; doi: 10.1073/pnas.0912157107.

Smith BA, Soderblom L, Batson R, *et al.* A new look at the Saturn system: The Voyager 2 images. *Science* 1982;215(4532):504–537; doi: 10.1126/science.215.4532.504.

Spengler B, Kirsch D, Kaufmann R, *et al.* Metastable decay of peptides and proteins in matrix-assisted laser-desorption mass spectrometry. *Rapid Commun Mass Spectrom* 1991;5(4):198–202; doi: 10.1002/rcm.1290050412.

Spengler B, Kirsch D, Kaufmann R, *et al.* Peptide sequencing by matrix-assisted laser-desorption mass spectrometry. *Rapid Commun Mass Spectrom* 1992;6(2):105–108; doi: 10.1002/rcm.1290060207.

Squyres SW, Reynolds RT, Cassen PM, *et al.* Liquid water and active resurfacing on Europa. *Nature* 1983;301:5897; doi: 10.1038/301225a0.

Sunner J, Dratz E, Chen Y-C. Graphite surface-assisted laser desorption/ionization time-of-flight mass spectrometry of peptides and proteins from liquid solutions. *Anal Chem* 1995;67(23):4335–4342; doi: 10.1021/ac00119a021.

Syka JEP, Coon JJ, Schroeder MJ, *et al.* Peptide and protein sequence analysis by electron transfer dissociation mass spectrometry. *Proc Natl Acad Sci USA* 2004;101(26):9528–9533; doi: 10.1073/pnas.0402700101.

Szczerbiński J, Metternich JB, Goubert G, *et al.* How peptides dissociate in plasmonic hot spots. *Small*, 2020;16(4):1905197; doi: 10.1002/smll.201905197.

Tanaka K, Waki H, Ido Y, *et al.* Protein and polymer analyses up to *m/z* 100 000 by laser ionization time-of-flight mass spectrometry. *Rapid Commun Mass Spectrom* 1988;2(8):151–153; doi: 10.1002/rcm.1290020802.

Teolis BD, Perry ME, Magee BA, *et al.* Detection and measurement of ice grains and gas distribution in the Enceladus plume by Cassini's Ion Neutral Mass Spectrometer. *J Geophys Res Space Physics* 2010;115(A9); doi: 10.1029/2009JA015192.

Theiling BP, Chou L, Da Poian V, *et al.* Science autonomy for ocean worlds astrobiology: A perspective. *Astrobiology* 2022;22(8):901–913; doi: 10.1089/ast.2021.0062.

Thomas PC, Tajeddine R, Tiscareno MS, *et al.* Enceladus's measured physical libration requires a global subsurface ocean. *Icarus*, 2016;264:37–47; doi: 10.1016/j.icarus.2015.08.037.

Valverde MA, García-Fernández T, Díaz-Cortés G, *et al.* Expanded use of a fast photography technique to characterize laser-induced plasma plumes. *Rev Mex Fis* 2014;60(3):195–204.

Waite JH, Combi MR, Ip W-H, *et al.* Cassini Ion and Neutral Mass Spectrometer: Enceladus plume composition and structure. *Science* 2006;311(5766):1419–1422; doi: 10.1126/science.1121290.

Waite JH, Glein CR, Perryman RS, *et al.* Cassini finds molecular hydrogen in the Enceladus plume: Evidence for hydrothermal processes. *Science* 2017;356(6334):155–159; doi: 10.1126/science.aai8703.

Wei J, Buriak JM, Siuzdak G. Desorption–ionization mass spectrometry on porous silicon. *Nature* 1999;399:6733; doi: 10.1038/20400.

Wen X, Dagan S, Wysocki VH. Small-molecule analysis with silicon-nanoparticle-assisted laser desorption/ionization mass spectrometry. *Anal Chem* 2007;79(2):434–444; doi: 10.1021/ac061154l.

Willhite L, Ni Z, Arevalo R, *et al.* CORALS: A laser desorption/ablation Orbitrap mass spectrometer for *in situ* exploration of Europa. In *2021 IEEE Aerospace Conference.* IEEE, Piscataway, NJ, 2021; doi: 10.1109/AERO50100.2021.9438221.

Wysocki VH, Tsaprailis G, Smith LL, *et al.* Mobile and localized protons: A framework for understanding peptide dissociation. *J Mass Spectrom* 2000;35(12):1399–1406; doi: 10.1002/1096-9888(200012)35:12<1399::AID-JMS86>3.0.CO;2-R.

Yergey AL, Coorssen JR, Backlund PS, *et al. De novo* sequencing of peptides using MALDI/TOF-TOF. *J Am Soc Mass Spectrom* 2002;13(7):784–791; doi: 10.1016/S1044-0305(02)00393-8.

Zenobi R, Knochenmuss R. Ion formation in MALDI mass spectrometry. *Mass Spectrom Rev* 1998;17(5):337–366; doi: 10.1002/(SICI)1098-2787(1998)17:5<337::AID-MAS2>3.0.CO;2-S.

Zhang Q, Zou H, Guo Z, *et al.* Matrix-assisted laser desorption/ionization mass spectrometry using porous silicon and silica gel as matrix. *Rapid Commun Mass Spectrom* 2001;15(3):217–223; doi: 10.1002/1097-0231(20010215)15:3<217::AID-RCM216>3.0.CO;2-I.

Address correspondence to:
Ziqin Ni
University of Maryland at College Park
8000 Regents Dr.
College Park, MD 20740
USA

E-mail: zni@umd.edu

Submitted 31 October 2022
Accepted 16 February 2023
Associate Editor: Nita Sahai

Abbreviations Used

AAG = Ala-Ala-Gly
CID = collision-induced dissociation
CORALS = Characterization of Ocean Residues and Life Signatures
*Cp*34H = *Colwellia psychrerythraea* strain 34H
ETD or ECD = electron transfer/capture dissociation
FFT = Fast Fourier Transform
GDAE = Gly-Asp-Ala-Glu
LDI = laser desorption/ionization
LDMS = laser desorption mass spectrometry
MALDI = matrix-assisted laser desorption/ionization
m/z = mass-to-charge ratio
SHD = Ser-His-Asp
SKSR = Ser-Lys-Ser-Arg
S/N = signal-to-noise ratio
UV = ultraviolet
UVPD = ultraviolet photodissociation